The Method of the Sensitivity Comparison of the Tin Dioxide Gas Sensor in Periodic Steady State

Libor GAJDOSIK

Department of Telecommunications, Faculty of Electrotechnical Engineering and Computer Science, VSB–Technical university of Ostrava, 17. listopadu 15, 708 33 Ostrava, Czech Republic

libor.gajdosik@vsb.cz

DOI: 10.15598/aeee.v15i3.2352

Abstract. *The formulas for the time dependency of the electrical conductivity of the sensor in thermal periodic steady state in the clean air atmosphere were derived herein. The created model of the sensor was experimentally verified and enables to compare the sensitivity to the tested substance at the frequencies at which the tests were carried out. The experiments were carried out with the sensors MQR 1003, SP 11, and TGS813. The sensors were tested in the clean air atmosphere and subsequently in the presence of ethanol, acetone and toluene vapour in the air at three different frequencies.*

Keywords

Semiconductor gas sensor, temperature modulation, thermal cycling, thermal inertia, tin dioxide.

1. Introduction

Sensors are often operated in periodic time variable heating regimes, because of better detection properties compared to the constant heating regime [1], [2], [3], [4], [5], [6], [7], [8], [9], [10], [11] and [12]. The overview of used types of time dependent heating of the sensor can be found in [13]. The theoretical models of the sensor response at the thermal modulation were presented in [14], [15], [16], [17], [18] and [19]. But in these works thermal inertia properties of the sensor were not considered. This is carried out herein. A heating system of the sensor has thermal inertia properties and that is why the detection properties of the sensor are dependent on the frequency of the heating voltage as well. The simple model of the behaviour of the sensor described herein can help to decide if the sensor is more or less sensitive to the given compound at given frequency.

2. Experiments

The commercial sensors of type MQR 1003, SP 11, and TGS 813 were operated in the clean air of 31 % relative humidity and then in the vapour of the single compound of concentration 100 ppm in the clean air. Ethanol, acetone, and toluene were used in the experiments. The sensor response, which is the electrical conductivity of the detection layer, was sensed in periodic steady state. The heating voltage was realized by a function in the following way:

$$U(t) = \sqrt{U_0 + U_A \sin(\omega t)}, \tag{1}$$

$$U_0 = \frac{U_M^2 + U_m^2}{2}, \qquad U_A = \frac{U_M^2 - U_m^2}{2}, \tag{2}$$

where t is the time, ω is the angular frequency, U_M is the maximum value of heating voltage and U_m is the minimum value of the heating voltage. For the experiments $U_M = 5$ V, $U_m = 2$ V. The response of the sensor was sampled in 32 points in every period of the heating voltage. The sampling rate t_s was chosen by experimental experience $t_s = 1000$ ms, $t_s = 500$ ms and $t_s = 200$ ms. Theses values are related to the frequencies of the sine component of the heating voltage $f = 0.0312$ Hz, $f = 0.0625$ Hz, $f = 0.156$ Hz, respectively.

3. Theory

A sensor consists of a heating system made of a heating resistance conductor covered by a ceramic insulator layer. The ceramic layer is covered by a metal oxide layer on which a pair of measuring electrodes is placed to measure the electrical conductivity of the metal oxide layer. The conductor is heated by an electrical voltage and heat penetrates through the ceramic layer into the detection layer. A gas detection does not occur until a specific temperature of the detection layer is reached, which is manifested by a change of the electrical conductivity of the detection layer. Each of these layers has its specific thermal properties. All these layers can be considered as one fictive layer of the thermal diffusivity a to simplify the mathematical solution. The heating voltage U generates the electrical power:

$$P = \frac{U^2}{R}, \tag{3}$$

where P is the electrical active power, R is the electrical resistance of the heating system of the sensor and U is the electrical voltage. This power is converted according to Joule - Lenz law into heat, which heats up the detection layer of the sensor to the temperature ϑ by the following formula:

$$Q = C\ \vartheta, \tag{4}$$

where C is the heat capacity of the system and Q is the Joule heat. It follows that the temperature ϑ is directly proportional to the Joule heat and consequently to the square power of the heating voltage U by the following formula:

$$\vartheta \approx \frac{1}{CR} U^2 = kU^2, \tag{5}$$

where k is the constant of proportionality. Substituting U from Eq. (1), we find:

$$\vartheta = kU^2 = k[U_0 + U_A \sin(\omega t)]. \tag{6}$$

Equation (6) can be rewritten into the following form:

$$\vartheta = \vartheta_0 + \vartheta_A \sin(\omega t)\ , \tag{7}$$

where ϑ_0 is the constant component and ϑ_A is the amplitude of the sine component of the driving temperature of the detection system of the sensor. Joule heat is conducted through the sensor and affects the temperature of the detection layer in the point x at the time t. This temperature can be designated as $\vartheta(x,t)$. But we do not measure the temperature $\vartheta(x,t)$ directly, we measure its manifestation, which is the electrical conductivity of the detection layer. The electrical conductivity of the detection layer is related to the temperature of the sensor according to [20] by the following formula:

$$G = G_0 \mathrm{e}^{-\frac{r}{\vartheta(x,t)}}, \tag{8}$$

where G_0 and r represent coefficients which are dependent on the material of the sensor and on the tested gas.

Heat conduction inside the layer can be solved by the Fourier - Kirchhoff equation. Heat conduction is considered in the halfplane $x > 0$ in the direction of the axis x:

$$a \frac{\partial^2 \vartheta}{\partial x^2} = \frac{\partial \vartheta}{\partial t}, \tag{9}$$

where a is the thermal diffusivity of the material ($\mathrm{m}^2 \cdot \mathrm{s}^{-1}$), ϑ is the temperature and t is the time. The heating system is supposed to be placed in the origin $x = 0$. We assume the initial condition in the following form to calculate the solution of Eq. (9) for sine component of Eq. (7):

$$\vartheta(0,t) = \vartheta_A \sin \omega t. \tag{10}$$

The periodical steady state solution is desired. The solution is supposed in the form as the product of two functions:

$$\vartheta(x,t) = g(x) \cdot f(t), \qquad \text{where } f(t) = \mathrm{e}^{j\omega t}. \tag{11}$$

Substituting Eq. (11) into Eq. (9) we obtain:

$$a \frac{\partial^2 g}{\partial x^2} \mathrm{e}^{j\omega t} = \frac{\partial}{\partial t} \left(g \mathrm{e}^{j\omega t} \right) = j\omega g \mathrm{e}^{j\omega t}. \tag{12}$$

Since the term $\exp(j\omega t)$ cancels on both sides of Eq. (12), we obtain:

$$a \frac{\mathrm{d}^2 g}{\mathrm{d}x^2} = j\omega g. \tag{13}$$

We rewrite Eq. (13) into the form:

$$\frac{\mathrm{d}^2 g}{\mathrm{d}x^2} - \frac{1}{a} j\omega g = 0. \tag{14}$$

We find the solution with the use of the relevant characteristic equation:

$$\lambda^2 - \frac{1}{a} j\omega = 0, \qquad \rightarrow \qquad \lambda^2 = j\frac{\omega}{a}. \tag{15}$$

The number λ equals:

$$\lambda_{1/2} = \pm \sqrt{j\frac{\omega}{a}} = \pm(1+j)\sqrt{\frac{\omega}{2a}} = \pm(1+j)h. \tag{16}$$

The solution of Eq. (13) equals:

$$g(x) = K_1 \mathrm{e}^{\lambda_1 x} + K_2 \mathrm{e}^{\lambda_2 x}. \tag{17}$$

Since $\vartheta(x,t) < \infty$ is valid, we consider the solution only in the form:

$$g(x) = K_1 \mathrm{e}^{\lambda_1 x}, \qquad \text{where} \qquad \lambda_1 = -(1+j)h\ . \tag{18}$$

Considering Eq. (11) the solution is written in the form:

$$\vartheta(x,t) = g(x) \cdot f(t) = K_1 \mathrm{e}^{-(1+j)hx} \mathrm{e}^{j\omega t}, \tag{19}$$

$$\vartheta(x,t) = K_1 \mathrm{e}^{-hx} \mathrm{e}^{j(-hx+\omega t)}. \tag{20}$$

Since the driving temperature $\vartheta(0,t)$ is expressed by a sine function, we consider only the sine component in the solution i.e. the imaginary part of Eq. (15). We can write:

$$\vartheta(x,t) = K_1 \mathrm{e}^{-hx} \sin(-hx + \omega t). \tag{21}$$

Regarding Eq. (10) in case that

$$K_1 = \vartheta_A, \tag{22}$$

it is necessary to modify the solution described by Eq. (21) for used experimental conditions. If $\omega = \infty$ in Eq. (21), it leads to $\exp(-hx) = 0$ and then $\vartheta(x,t) = 0$. The sensor heated by the voltage described by Eq. (1) reaches non-zero temperature at the frequency $\omega = \infty$. This is why Eq. (21) is to be modified by introducing the constant ϑ_0. We obtain:

$$\vartheta(x,t) = \vartheta_0 + \vartheta_A \mathrm{e}^{-hx} \sin(-hx + \omega t). \tag{23}$$

Equation (23) is also the solution of Eq. (9), because Eq. (23) contains only additional constant ϑ_0 compared to Eq. (21). If the heating voltage is described by Eq. (1), the temperature of the detection layer in the place x at the time t is described by Eq. (23). With the use of Eq. (7) we obtain the conductivity of the detection layer in the following form:

$$\begin{aligned} &G(t) = G_0 \mathrm{e}^{-\frac{r}{\vartheta(x,t)}}, \qquad \text{where} \\ &\vartheta(x,t) = \vartheta_0 + \vartheta_A \mathrm{e}^{-hx} \sin(-hx + \omega t). \end{aligned} \tag{24}$$

The term hx can be modified with the use of Eq. (16) and Eq. (23) into the following form:

$$hx = x\sqrt{\frac{\omega}{2a}} = x\sqrt{\frac{\pi f}{a}} = h_1\sqrt{f}, \qquad h_1 = x\sqrt{\frac{\pi}{a}}. \tag{25}$$

The coefficient h_1 is dependent on the construction of the sensor, x is the thickness of the heated fictive layer. Then it is possible to write the electrical conductivity of the sensor in the following form:

$$\begin{aligned} &G(t) = \mathrm{e}^{-\frac{1}{\vartheta(x,t)}}, \qquad \text{where} \\ &\vartheta(t) = A + B\mathrm{e}^{-h_1\sqrt{f}} \sin(-h_1\sqrt{f} + 2\pi\sqrt{f}t), \end{aligned} \tag{26}$$

where the constants A, B and h_1 can be determined from experimental data. This function can be used for approximation of experimental values of the electrical conductivity of the detection layer. The choice of the constants $G_0 = r = 1$ is admissible from the mathematical point of view to reach the equality of $G(t)$ between Eq. (26) and Eq. (24).

The heating voltage $U(t)$ and the electrical conductivity $G(t)$ are periodical functions, whose periodicity is determined by the sine function. Maxima and minima of $G(t)$ and $U(t)$ appear when the sine equals ± 1. When concidering following in Eq. (1):

$$\omega t_i = (2n+1)\frac{\pi}{2}, \qquad n = 0,\ 1,\ 2, \ldots, \tag{27}$$

then the maxima of the heating voltage $U(t)$ occur in the time t_i. When concidering following in Eq. (24):

$$-h_1\sqrt{f} + \omega t_j = (2n+1)\frac{\pi}{2}, \qquad n = 0,\ 1,\ 2, \ldots, \tag{28}$$

then the maxima of the electrical conductivity $G(t)$ occur at the time t_j. It follows from Eq. (27) and Eq. (28), that the following equation must be satisfied for two matching maxima of $U(t_i)$ and $G(i_j)$:

$$-h_1\sqrt{f} + \omega t_j = \omega t_i. \tag{29}$$

We express from Eq. (29):

$$h_1 = \frac{\omega t_j - \omega t_i}{\sqrt{f}} = 2\pi\sqrt{f}(t_j - t_i) = 2\pi\Delta t\sqrt{f}, \tag{30}$$

where Δt is the time delay between the heating voltage and the electrical conductivity. Δt can be calculated from the experimental values of $G(t)$ and $U(t)$. Then h_1 can be calculated from Eq. (30).

We designate in Eq. (26), that:

$$u = \mathrm{e}^{-h_1\sqrt{f}}. \tag{31}$$

With the use of Eq. (26) and Eq. (31), the following expressions can be defined as:

$$G_M = \mathrm{e}^{-\frac{1}{A+Bu}}, \qquad G_m = \mathrm{e}^{-\frac{1}{A-Bu}}, \tag{32}$$

where G_M represents the maximum and G_m represents the minimum value of the electrical conductivity. The constants A and B can be expressed from Eq. (32). Substituting u from Eq. (31) we obtain:

$$A = \frac{1}{2}\left(\frac{1}{-\ln G_M} + \frac{1}{-\ln G_m}\right), \tag{33}$$

$$B = \frac{1}{2}\left(\frac{1}{-\ln G_M} - \frac{1}{-\ln G_m}\right)\mathrm{e}^{h_1\sqrt{f}}. \tag{34}$$

Equation (33) and Eq. (34) enable to calculate A and B from the experimental values of G_M and G_m. The coefficient h_1 is calculated by Eq. (30).

The percent deviation δ was defined by the following formula:

$$\delta = \frac{S_e - S_a}{S_a} \cdot 100, \tag{35}$$

where S_e is the difference $S_e = G_M - G_m$ taken from the experimental values and S_a is the difference $S_a = G_M^{'} - G_m^{'}$, where $G_M^{'}$ and $G_m^{'}$ designate the theoretical values given by Eq. (26). The quantity S_e we can also call the swing of the experimental sine component whereas S_a the swing of the theoretical sine component. The quantity δ enables to compare magnitudes of the alternating sine components of the sensor response at given frequency.

4. Results

The values of the time difference Δt were found in the experimental values of the measurement carried out in the clean air. It was found, that the maximum of G is delayed behind the maximum of $U(t)$ as expected according to heat conduction theory. The value h_1 was calculated from Eq. (30). The overview of the calculated values is in Tab. 1.

Tab. 1: The experimental values of the sensor in the clean air.

f (Hz)	Δt (s)	h_1 ($\mathrm{m^2 \cdot s^{-1} \cdot K^{-1}}$)	**Average of h_1**
MQR 1003			
0.0312	4.0	4.442	
0.0625	3.0	4.712	4.209
0.156	1.4	3.474	
SP 11			
0.0312	1.0	1.110	
0.0625	1.5	2.356	1.982
0.156	1.0	2.481	
TGS 813			
0.0312	3.0	3.332	
0.0625	2.5	3.926	3.577
0.156	1.4	3.474	

The constants A and B were calculated from Eq. (33) and Eq. (34) at the frequency $f = 0.0312$ Hz with the use of the average value of h_1 from Tab. 1. When two near maxima of G_M or two near minima of G_m occurred, their average value was used instead them. The calculated values are in Tab. 2.

Tab. 2: The coefficients of the sensor in the clean air at the frequency $f = 0.0312$ Hz.

G_M (μS)	G_m (μS)	$A \cdot 10^2$ (1)	$B \cdot 10^2$ (1)
MQR 1003			
10.12	0.29	7.668	2.159
SP 11			
9.82	0.30	7.665	1.429
TGS 813			
10.07	0.49	7.810	1.745

The data in Tab. 2 were considered as input data used in Eq. (26) and only the frequency f was changed. Then Eq. (26) was used as the model of behaviour of the sensor.

An example of the results is in Fig. 1, Fig. 2 and Fig. 3. At the beginning the theoretical curves were calculated at the frequency $f = 0.0312$ Hz. The curves fit the experimental data well. The example is in Fig. 1. The accordance is a bit worse in Fig. 2, where the frequency $f = 0.0625$ Hz was used. The curve is even shifted compared to the measured data in Fig. 3, where the frequency $f = 0.156$ Hz was used. Heat is conducted from the heating system faster into the sensor compared to convection of heat away of the sensor into its surrounding at higher frequency. This phenomenon can elevate the temperature of the sensor and shift the theoretical curve compared to measured data. The heat exchange between the sensor and its surrounding was not considered in the derivation of Eq. (26). Despite this the neglecting of the phenomenon is acceptable for the purpose of which Eq. (26) is used herein.

Table 3 includes the deviation δ calculated for the clean air. From it follows that the deviation δ does not exceed 23 %.

The sensors were further tested in the concentration $x = 100$ ppm of the single tested vapour in the air at the same heating voltage as in the clean air case. The conductivities G_M and G_m were found out in the experimental data of the tested vapour and average of h_1 from Tab. 1 was used to calculate the constants A and B with the use of Eq. (33) and Eq. (34) at the frequency

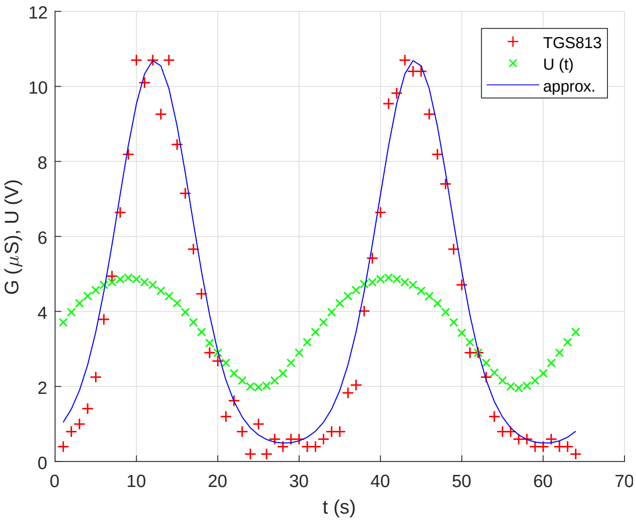

Fig. 1: The electrical conductivity $G(t)$ of the sensor TGS 813 at frequency $f = 0.0312$ Hz in the clean air. $U(t)$ is the heating voltage.

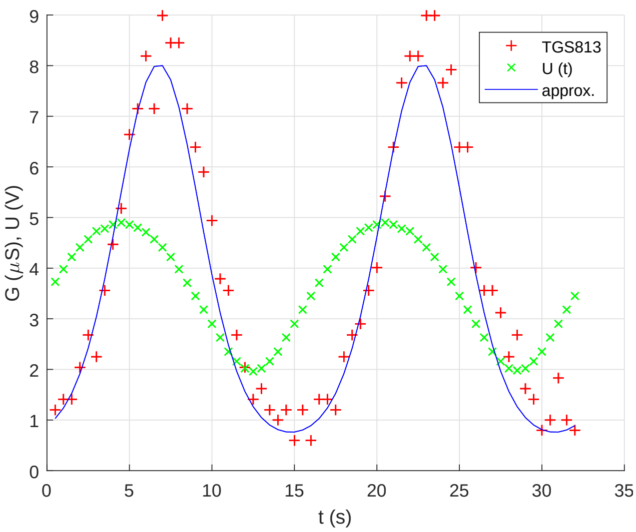

Fig. 2: The electrical conductivity $G(t)$ of the sensor TGS 813 at frequency $f = 0.0625$ Hz in the clean air. $U(t)$ is the heating voltage.

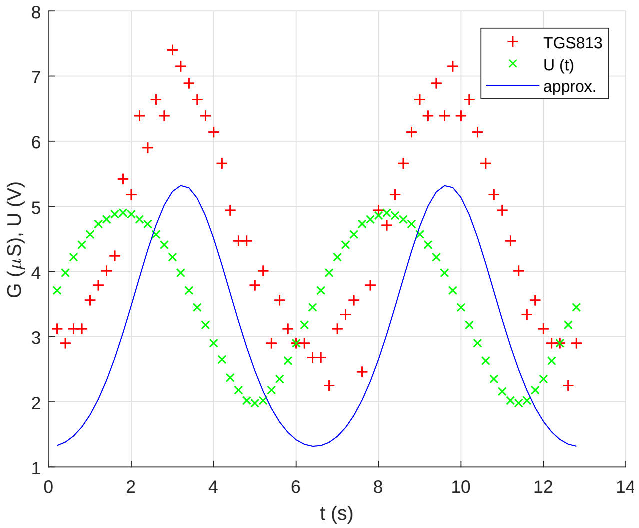

Fig. 3: The electrical conductivity $G(t)$ of the sensor TGS 813 at frequency $f = 0.156$ Hz in the clean air. $U(t)$ is the heating voltage.

Tab. 3: The deviations of δ in % for the sensors in clean air at the used frequencies.

f=0.0312 Hz	f=0.0625 Hz	f=0.156 Hz
MQR 1003		
3.04	-1.8	2.5
SP 11		
2.0	2.0	14.5
TGS 813		
1.5	17.2	23.0

$f = 0.0312$ Hz. These constants were used to calculate the reference curve by Eq. (26) and subsequently the deviation δ by Eq. (35) at all the frequencies. Table 4 includes the results.

Tab. 4: The values of δ in % for the sensor in the tested vapours.

	f=0.0312 Hz	f=0.0625 Hz	f=0.156 Hz
acetone			
MQR 1003	0.5	12.9	59.9
SP 11	2.7	-51.6	-62.4
TGS 813	4.0	-19.5	-27.4
ethanol			
MQR 1003	0.8	46.3	53.8
SP 11	5.4	-14.6	-42.2
TGS 813	0.9	6.7	-25.3
toluene			
MQR 1003	0.5	10.9	-45.7
SP 11	7.6	-54.7	-79.7
TGS 813	7.5	-37.8	-42.1

The deviations δ in the column at the frequency $f = 0.0312$ Hz are small, because of the constants A and B which were calculated from the experimental data at this frequency. This represents the reference column. The results in Tab. 4 show that the swing of the conductance of the sensor MQR 1003 is greater by 59.9 % at the frequency $f = 0.156$ Hz for the acetone case than expected. Similarly it is for the case when ethanol was used at the frequencies $f = 0.625$ Hz and $f = 0.156$ Hz. On the other hand the sensor SP 11 indicates for the acetone case and for the toluene case the swing smaller by -51.6 % or even less at the frequencies $f = 0.0625$ Hz and $f = 0.156$ Hz then expected. It follows that the parameter δ can serve as a decision criterion if the sensor is more or less sensitive to the compound at given frequency compared to the expected value. The curve calculated by Eq. (26) can be considered as a reference curve for which the parameter δ is calculated by Eq. (35).

An example of measured data and the dependency of Eq. (26) is in Fig. 4, Fig. 5, and Fig. 6. For the measured data, the maximum of G is not always delayed behind the maximum of $U(t)$ as expected when a compound is detected. That is why the method of the calculation of h_1 by Eq. (30) fails here. The coefficient h_1 is related to the thermal properties of the sensor and it would be independent on a detected compound. The correct value of h_1 can be calculated when the experimental data of the clean air are taken.

It is general knowledge [21], [22] and [23], that during the detection of ethanol the maximum of the electrical conductance occurs at specific heating voltage between the values $U = 2$ V and 5 V. Hence the maximum of $G(t)$ for the ethanol case occurs earlier than the maximum of $G(t)$ for the clean air case. The corollary of this is less or even a negative delay Δt between $G(t)$ and $U(t)$. The phenomenon can be seen in Fig. 4, Fig. 5 and Fig. 6. Ethanol is not only one compound with maximum electrical conductance at specific heating voltage and the negative delay Δt can occur also during the test of other substances.

It follows from Eq. (26) that for $f = \infty$, the magnitude of the sine component tends to zero. The value

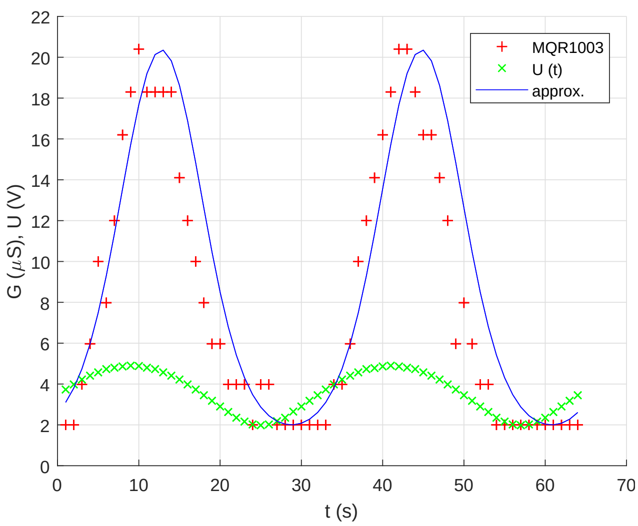

Fig. 4: The electrical conductivity $G(t)$ of the sensor MQR 1003 for ethanol of the concentration $x = 100$ ppm at frequency $f = 0.0312$ Hz of the heating voltage. $U(t)$ is the heating voltage.

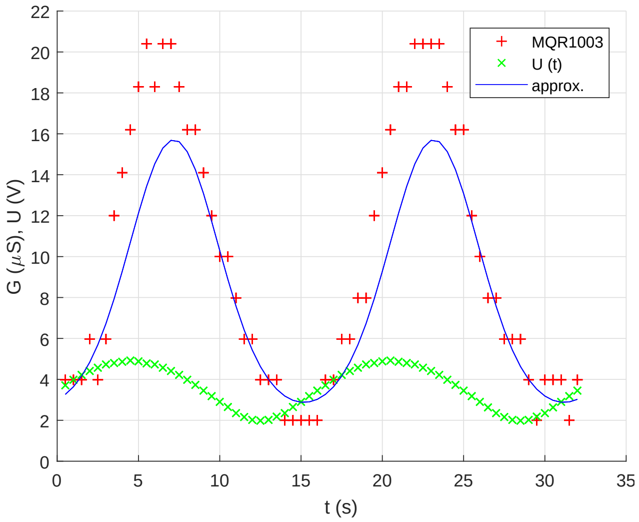

Fig. 5: The electrical conductivity $G(t)$ of the sensor MQR 1003 for ethanol of the concentration $x = 100$ ppm at frequency $f = 0.0625$ Hz of the heating voltage. $U(t)$ is the heating voltage.

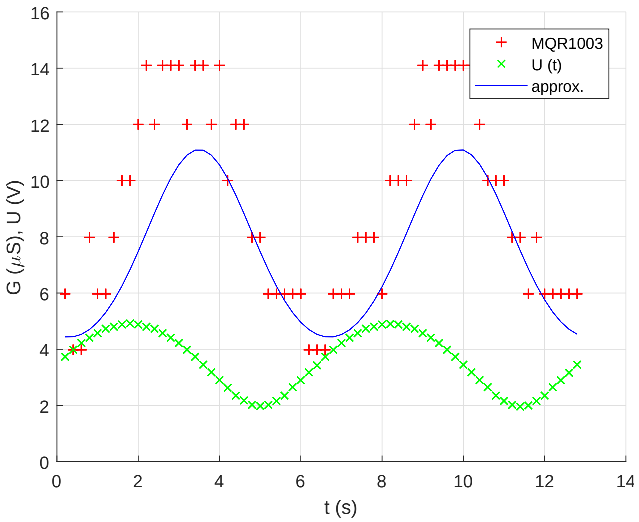

Fig. 6: The electrical conductivity $G(t)$ of the sensor MQR 1003 for ethanol of the concentration $x = 100$ ppm at frequency $f = 0.156$ Hz of the heating voltage. $U(t)$ is the heating voltage.

of the electrical conductivity $G(t)$ becomes time independent despite the time dependent heating. The electrical conductivity tends to the value as if the sensor were heated by the specific constant voltage. It is possible, using Eq. (31), Eq. (32), Eq. (33) and Eq. (34), to calculate the frequency at which the amplitude of the sine component of the electrical conductivity reaches the prescribed value. The values of δ in Tab. 4 indicate great positive or negative deviations compared to the expected value. It means that the decay of the swing of the sine component is not monotonous in the presence of the detected substance as theoretically expected and the prediction of such a frequency can be carried out only experimentally for the tested compound.

5. Conclusion

The electrical conductivity of the tin dioxide gas sensor was derived herein. The model of the sensor is based on thermal inertia and it is valid for specific periodical heating voltage. The model was verified with the experimental data. It was found that the model can be used in the determination of sensitivity of the sensor to the tested substance at given frequency.

Acknowledgment

This study was enabled due to Project TA04021263 entitled The Intelligent Modules for Communication and Lightening provided by TACR (The Technology Czech Science Foundation) and due to Project FV10369 SIDAS entitled The System of Inelligent Detection and Signaling of Clashing States for Improvement the Truck Safety provided by The Ministry of Industry and Trade. Further this article was prepared within the frame of sustainability of the project No. CZ.1.07/2.3.00/20.0217 "The Development of Excellence of the Telecommunication Research Team in Relation to International Cooperation" within the frame of the operation programme "Education for competitiveness" that was financed by the Structural Funds and from the state budget of the Czech Republic.

References

[1] XINGJIU, H., J. S. DONGLIANG, P. ZONXIN and Y. ZENGLIANG. Rectangular mode of operation for detecting pesticide residue by using a single SnO_2-based gas sensor. *Sensors and Actuators B: Chemical*. 2003, vol. 96, iss. 3, pp. 630–635. ISSN 0925-4005. DOI: 10.1016/j.snb.2003.07.006.

[2] XINGJIU, H., M. FANLI, P. ZONGXIN, X. WEIHONG and L. JINHUAI. Gas sensing behavior of a single tin dioxide sensor under dynamic temperature modulation. *Sensors and Actuators B: Chemical*. 2004, vol. 99, iss. 2–3, pp. 444–450. ISSN 0925-4005. DOI: 10.1016/j.snb.2003.12.013.

[3] HERRERO-CARON, F., D. J. YANEZ and F. DE BORJA RODRIGUEZ. An active, inverse temperature modulation strategy for single sensor odorant classification. *Sensors and Actuators B: Chemical*. 2015, vol. 206, iss. 1, pp. 555–563. ISSN 0925-4005. DOI: 10.1016/j.snb.2014.09.085.

[4] NAKATA, S., H. NAKAMURA and K. YOSHIKAWA. New strategy for the development of a gas sensor based on the dynamic

characteristics: principle and preliminary experiment. *Sensors and Actuators B: Chemical*. 1992, vol. 8, iss. 2, pp. 187–189. ISSN 0925-4005. DOI: 10.1016/0925-4005(92)80179-2.

[5] NAKATA, S., K. TAKEMURA and K. NEYA. Non-linear dynamic responses of a semiconductor gas sensor: Evaluation of kinetic parameters and competition effect on the sensor response. *Sensors and Actuators B: Chemical*. 2001, vol. 76, iss. 1–3, pp. 436–441. ISSN 0925-4005. DOI: 10.1016/S0925-4005(01)00652-9.

[6] NAKATA, S., H. OKUNISHI and Y. NAKASHIMA. Distinction of gases with a semiconductor sensor under a cyclic temperature modulation with second-harmonic heating. *Sensors and Actuators B: Chemical*. 2006, vol. 119, iss. 2, pp. 556–561. ISSN 0925-4005. DOI: 10.1016/j.snb.2006.01.009.

[7] JAEGLE, M., J. WOLLENSTEIN, T. MEISINGER, H. BOTTNER, G. MULLER, T. BECKER and C. BOSCH-BRAUNMUHL. Micromachined thin film SnO_2 gas sensors in temperature-pulsed operation mode. *Sensors and Actuators B: Chemical*. 1999, vol. 57, iss. 1–3, pp. 130–134. ISSN 0925-4005. DOI: 10.1016/S0925-4005(99)00074-X.

[8] HEILIG, A., N. BARSAN, U. WEIMAR, M. SCHWEIZER-BERBERICH, J. W. GARDNER and W. GOPEL. Gas identification by modulating temperatures of SnO_2-based thick film sensors. *Sensors and Actuators B: Chemical*. 1997, vol. 43, iss. 1–3, pp. 45–51. ISSN 0925-4005. DOI: 10.1016/S0925-4005(97)00096-8.

[9] VERGARA, A., E. LLOBET, J. BREZMES, P. IVANOV, C. CANE, I. GRACIA, X. VILANOVA and X. CORREIG. Quantitative gas mixture analysis using temperature-modulated micro-hotplate gas sensors: Selection and validation of the optimal modulating frequencies. *Sensors and Actuators B: Chemical*. 2007, vol. 123, iss. 2, pp. 1002–1016. ISSN 0925-4005. DOI: 10.1016/j.snb.200.

[10] ILLYASKUTTY, N., J. KNOBLAUCH, M. SCHWOTZER and H. KOHLER. Thermally modulated multi sensor arrays of SnO_2/additive/electrode combinations for enhanced gas identification. *Sensors and Actuators B: Chemical*. 2015, vol. 217, iss. 1, pp. 2–12. ISSN 0925-4005. DOI: 10.1016/j.snb.2015.03.018.

[11] HOSSEIN-BABAEI, F. and A. AMINI. A breakthrough in gas diagnosis with a temperature-modulated generic metal oxide gas sensor. *Sensors and Actuators B: Chemical*. 2012, vol. 166–167, iss. 1, pp. 419–425. ISSN 0925-4005. DOI: 10.1016/j.snb.2012.02.082.

[12] IONESCU, R. and E. LLOBET. Wavelet transform-based fast feature extraction from temperature modulated semiconductor gas sensors. *Sensors and Actuators B: Chemical*. 2002, vol. 81, iss. 2–3, pp. 289–295. ISSN 0925-4005. DOI: 10.1016/S0925-4005(01)00968-6.

[13] LEE, A. P. and B. J. REEDY. Temperature modulation in semiconductor gas sensing. *Sensors and Actuators B: Chemical*. 1999, vol. 60, iss. 1, pp. 35–42. ISSN 0925-4005. DOI: 10.1016/S0925-4005(99)00241-5.

[14] IONESCU, R., E. LLOBET, S. AL-KHALIFA, J. W. GARDNER, X. VILANOVA, J. BREZMES and X. CORREIG. Response model for thermally modulated tin-oxide absed microhotplate gas sensors. *Sensors and Actuators B: Chemical*. 2003, vol. 95, iss. 1–3, pp. 203–211. ISSN 0925-4005. DOI: 10.1016/S0925-4005(03)00420-9.

[15] FORT, A., S. ROCCHI, M. B. SERRANO-SANTOS, M. MUGNAINI, V. VIGNOLI, A. ATREI and R. SPINICCI. CO sensing with SnO_2 based thick film sensors: Surface state model for conductance responses during thermal modulation. *Sensors and Actuators B: Chemical*. 2006, vol. 116, iss. 1–2, pp. 43–48. ISSN 0925-4005. DOI: 10.1016/j.snb.2005.11.070.

[16] DING, J., T. J. MCAVOY, R. E. CAVICCHI and S. SEMANCIK. Surface state trapping models for SnO_2-based microhotplate sensors. *Sensors and Actuators B: Chemical*. 2001, vol. 77, iss. 3, pp. 597–613. ISSN 0925-4005. DOI: 10.1016/S0925-4005(01)00765-1.

[17] KUNT, T., T. MCAVOY, R. E. CAVICCHI and S. SEMANCIK. Optimization of temperature programmed sensing for gas identification using micro-hotplate sensors. *Sensors and Actuators B: Chemical*. 1998, vol. 53, iss. 1–2, pp. 24–43. ISSN 0925-4005. DOI: 10.1016/S0925-4005(98)00244-5.

[18] GOSANGI, R. and R. GUTIERREZ-OSUNA. Active temperature modulation of metal-oxide sensors for quantitative analysis of gas mixtures. *Sensors and Actuators B: Chemical*. 2013, vol. 185, iss. 1, pp. 201–210. ISSN 0925-4005. DOI: 10.1016/j.snb.2013.04.056.

[19] MARTINELLI, E., D. POLESE, A. CATINI, A. D'AMICO and C. DI NATALE. Self-adapted temperature modulation in metal-oxide semiconductor gas sensors. *Sensors and Actuators B: Chemical*. 2012, vol. 161, iss. 1–3, pp. 534–541. ISSN 0925-4005. DOI: 10.1016/j.snb.2011.10.072.

[20] MORRISON, S. R. Semiconductor gas sensors. *Sensors and Actuators B: Chemical*. 1981–1982, vol. 2, iss. 1, pp. 329–341. ISSN 0925-4005. DOI: 10.1016/0250-6874(81)80054-6.

[21] SINGH, R. C., N. KOHLI, N. P. SINGH and O. SINGH. Ethanol and LPG sensing characteristics of SnO_2 activated Cr_2O_3 thick film sensor. *Bulletin of Materials Science*. 2010, vol. 33, iss. 5, pp. 575–579. ISSN 0250-4707.

[22] SCHMID, W., N. BARSAN and U. WEIMAR. Sensing of hydrocarbons with tin oxide sensors: possible reaction path as revealed by consumption measurements. *Sensors and Actuators B: Chemical*. 2003, vol. 89, iss. 3, pp. 232–236. ISSN 0925-4005. DOI: 10.1016/S0925-4005(02)00470-7.

[23] HAE-WON, C. and L. MAN-JONG. Sensing characteristics and surface reaction mechanism of alcohol sensors based on doped SnO_2. *Journal of Ceramic Processing Research*. 2006, vol. 7, iss. 3, pp. 183–191. ISSN 1229-9162.

About Authors

Libor GAJDOSIK graduated in telecommunication engineering from the Czech Technical University (Prague, Czech Republic) in 1983. He received his Ph.D. in 1998 from the VSB–Technical University of Ostrava (Ostrava, Czech Republic). His thesis was focused on the detection properties of tin dioxide gas sensors at the dynamic operating modes. He has been an assistant professor at the Technical University of Ostrava since 1989. His main interests are electronics, circuit theory and chemical sensors.